Calculation of Response matrix of a BSS with ^{6}LiI scintillator

H.R. Vega-Carrillo[*,a,b], I. Donaire[c], E. Gallego[c], E. Manzanares-Acuña[a], A. Lorente[c], M.P. Iñiguez[d], A. Martin-Martin[d], and J.L. Gutierrez-Villanueva[d]

[a] *Unidades Academicas de Estudios Nucleares e Ingenieria Electrica[b], Universidad Autónoma de Zacatecas, apartado postal # 336, 98000 Zacatecas, Zac. Mexico.*

[c] *Departamento de Ingeniería Nuclear de la Universidad Politécnica de Madrid, Spain.*

[d] *Departamento de Fisica Teorica, Atomica y Optica, Laboratorio LIBRA de la Universidad de Valladolid, Spain*

Recibido el 14 de mayo de 2007; aceptado el 26 de octubre de 2007

The response matrix of a Bonner sphere spectrometer was calculated using MCNP 4C and MCNPX 2.4.0 codes. As thermal neutron detector a 0.4 cm $\times\emptyset$ 0.4 cm ^{6}LiI which is located at the center of a set of polyethylene spheres. The response was calculated for 0, 2, 3, 5, 8, 10, and 12 inches-diameter polyethylene spheres for neutrons whose energy goes from 2.50E(-8) to 100 MeV. The response matrix was calculated for 23 neutron energies, the response functions were energy-interpolated to 51 neutron energies and were compared with a matrix response reported in the literature, in this comparison both response matrices are in agreement. The main differences were found in the bare detector and are attributed to the irradiation conditions and cross sections, for the other detectors the differences are due to the cross sections libraries.

Keywords: Monte Carlo; ^{6}LiI scintillator; Bonner sphere neutron spectrometer.

Se calculó la matriz de respuesta de un espectrómetro de Esferas de Bonner utilizando los códigos Monte Carlo MCNP 4C y MCNPX 2.4.0. El detector de neutrones térmicos del espectrómetro es un centellador cilíndrico, 0.4 cm $\times\emptyset$ 0.4 cm, de ^{6}LiI, que se ubica en el centro de esferas de polietileno. La respuesta se obtuvo para esferas cuyo diámetro es 0, 2, 3, 5, 8, 10 y 12 pulgadas y para fuentes monoenergéticas de neutrones de 2.50E(-8) to 100 MeV. La matriz se calculó para 23 fuentes monoenergéticas, las funciones de respuesta se interpolaron a 51 energías que se compararon con las correspondientes reportadas en la literatura. Se encontró que ambas matrices son coincidentes, excepto para neutrones de baja y alta energía; esta diferencia es atribuida a las condiciones de irradiación utilizadas en ambos estudios y a las secciones eficaces.

Descriptores: Monte Carlo; centellador ^{6}LiI; espectrómetro de esferas de Bonner.

PACS: 24.10.Lx; 29.40.Mc; 29.30.-h

1. Introduction

Since the demonstration of neutron existence by Chadwick in 1932 [1], these neutral particles have become an important tool in several fields such as nuclear technology, nuclear physics, fusion plasma diagnostics, radiotherapy, and radiation protection.

In 1960 the multisphere spectrometer, also known as Bonner sphere spectrometer (BSS), was introduced in the aim to measure the neutron energy distribution, known as neutron spectrum [2]. BSS is a set of polyethylene spheres with different diameters with a thermal neutron detector that is located at the centre of the spheres. Because the spherical shape the response of BSS is isotropic.

From 1960 to 1979 several advances in computer unfolding methods, the application of semiconductor detectors to neutron spectrometry and the introduction of superheated drop detectors contributed to progress in neutron spectrometry [3].

With the BSS the neutron spectra is obtained in a wide range of energies ranging from thermal up to at least 20 MeV [4]. By adding intermediate shells of lead to the moderator spheres the BSS is utilized to measure neutrons reaching few GeV [5,6].

Different materials had been utilized as thermal neutron detector in the BSS such as, ^{6}LiI(Eu) scintillator [2,7], pairs of thermoluminiscent dosimeters (TLD600-TLD700) [8–10], gold and other activation foils [11], track detectors [12], BF_3[13] or ^{3}He [14] filled proportional counters. When the detector is located inside the polyethylene spheres the response is modified due to the moderating effect of the spheres. The set of responses are named response matrix [6,15].

Inside a neutron field the detector, bare o inside of any sphere, produces a count rate; the detectors' count rates (C) are related with the response matrix (R_Φ (E)) and the neutron spectrum (Φ_E(E)) through the Fredholm integral equation of the first kind, shown in Eq. (1).

$$C = \int_{E_i}^{E_f} R_\Phi(E)\,\Phi_E(E)dE \tag{1}$$

Once Eq. (1) is solved and the neutron spectrum is known the neutron dose, Δ can be estimated using Eq. (2) [16].

$$\Delta = \int_{E_i}^{E_f} \delta_\Phi(E)\,\Phi_E(E)\,dE \tag{2}$$

Here, δ_Φ (E) is the fluence-to-dose conversion coefficient. Depending of the type of δ_Φ (E) utilized any type of neutron dose can be estimated.

Technological limitations prevent the experimental determination of the response matrix utilizing monoenergetic neutrons. However, this is only practical for few monoenergetic

neutrons with energies greater than about a few keV and for thermal neutrons [6]. Therefore the responses need to be calculated; this has been realized using the one-dimensional discrete ordinates transport code ANISN [17], Monte Carlo methods with the MCNP code [18,19], MCNPX code [14], and high-energy codes [5].

In this investigation the response matrix of a Bonner spectrometer with a ^{6}LiI scintillator has been calculated using Monte Carlo methods with updated cross section libraries. This matrix was interpolated to include a larger number of energy bins and it was compared with the response matrix reported in the literature.

2. Methods

Naturally occurring Li isotopes are 92.5% Li-7 and 7.5% Li-7, while I has only one natural isotope I-127; all those isotopes are stable. The ^{6}LiI(Eu) scintillator has Li-6, Li-7, I-127 isotopes, smaller amounts of Eu are added as impurities. The cross sections of isotopes are shown in Fig. 1 [20]. When neutrons reach the scintillator some are absorbed by the different nuclei in the detector. For each nuclei species the number of absorption, n_a, are estimated with Eq. (3).

$$n_a = \int_{V_{LiI}} d^3r \int_E \Phi_E(r,E) \sum\nolimits_a (r,E)\, dE \qquad (3)$$

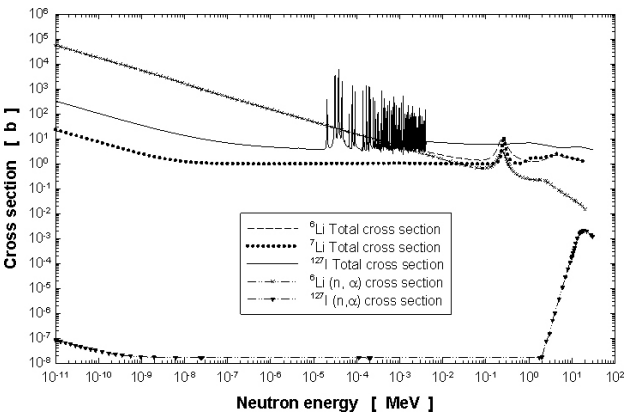

FIGURE 1. Cross sections of scintillator isotopes.

Here, the integration volume is taken over the LiI scintillator volume, Φ_E(r, E) is the position and energy dependent neutron flux, and Σ_a(r, E) is the macroscopic absorption cross section. Some of these absorptions will induce the reaction (n, α). For the ^{6}LiI(Eu) scintillator the cross section that significantly contributes to the number of neutron absorptions is the ^{6}Li absorption cross section.

A realistic model of the detector, including the 0.4 cm × 0.4 ∅ cm ^{6}LiI scintillator, the light pipes and the detector's cask, and the polyethylene spheres were designed. The calculated cases were the bare detector (Ball 0) and those with the detector inserted in the spheres of 2" (Ball 2), 3" (Ball 3), 5" (Ball 5), 8" (Ball 8), 10" (Ball 10) and 12" (Ball 12). In the model design the light pipes were modeled as made of polymethyl methacrylate, the cask was modeled as made of aluminum and the scintillator was modeled as made of ^{6}Li, ^{7}Li and I; the Eu impurities were excluded.

Each model was irradiated with a parallel neutron beam produced by a disk-shaped neutron source; irradiations were carried out using 20 monoenergetic neutrons for each detector. The energy of the monoenergetic neutron sources varied from 2.50E(-8) to 20 MeV. These calculations were performed with the Monte Carlo code MCNP 4C [21] and the ENDF/B-VI cross section library [22].

Using MCNPX [23], version 2.4.0, the response calculations were extended until 100 MeV neutrons using the LA150 cross section library [24]. In all calculations the response was defined as the number of ^{6}Li(n, α)^{3}H reactions occurring in the scintillator per each neutron emitted by the disk-shaped monoenergetic neutron source.

In calculations reported in literature the scintillator has been modeled with different mass densities: 3.84 g-cm^3 [18], 4.08 g-cm^3 [25]; it was also assumed that the enrichment of ^{6}Li is 100% [18] and 96.1% [25], these assumptions give an atomic density in the scintillator of 1.74E(22) [18] and 1.848E(22) [25] atoms-cm^{-3}.

In this investigation the scintillator was modeled using a density of 3.494 g-cm^{-3} and composed by 4.36 w/o of ^{6}Li, 0.18 w/o of ^{7}Li and 95.46 w/o of I. These characteristics give an atomic density of the scintillator of 3.162E(22) atoms-cm^{-3}.

Moderating spheres were modeled with a density of 0.95 g-cm^{-3} and made of polyethylene. Atomic composition and physical data of different elements utilized to build the model were obtained from Seltzer and Berger [26].

Chemical binding and crystalline effects of polyethylene during thermal neutron scattering were taken into account using the S(α, β) treatment [21]. A disk-shaped source term with the same diameter as the moderating sphere was used to represent a monoenergetic neutron source whose neutrons were directed towards the polyethylene sphere.

Polyethylene spheres were modeled as a series of concentric polyethylene shells, each with a different neutron importance, increasing as the sphere center was approached. This was the only variance reduction technique used in the calculations. Throughout the MCNP 4C and MCNPX calculations the number of histories used for each sphere was large enough to have uncertainties less than 3%. The calculated responses were interpolated to include a larger number of energy bins.

3. Results and discussion

In Fig. 2 the response functions for 0, 2, 3, 5, 8, 10, and 12 inches-diameter polyethylene spheres as a function of neutron energy are shown. The bare detector (Ball 0) has the shape of ^{6}Li cross section. As the sphere's diameter is increased the response tends to decrease for thermal and epithermal neutrons. On the other hand, the maximum in the

responses is shifted to higher energies for large spheres. This is in agreement with the response matrix reported in the literature [17,18] even regardless the type of thermal neutron detector [12,15].

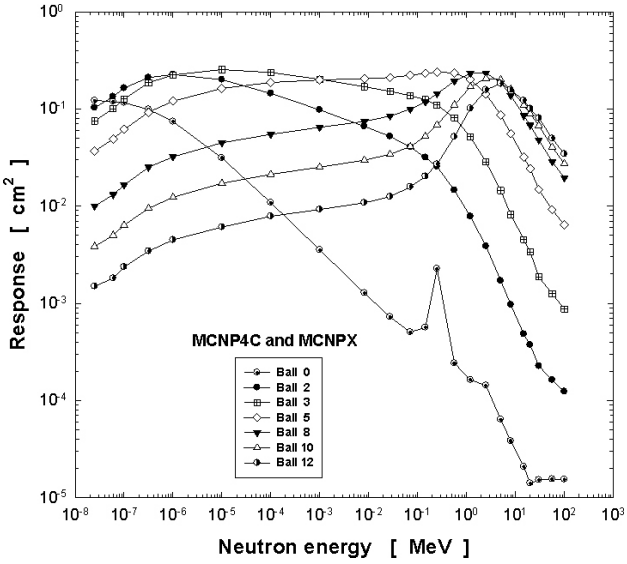

FIGURE 2. MCNP4C and MCNPX calculated response matrix for BSS with ^{6}LiI detector.

The energy-interpolated response matrix is shown in Fig. 3, and their values are shown in Table I. Energy-interpolated response functions were compared with those published by Mares and Schraube [18]. In Figs. 2 and 3 can be noticed that the bare response function, strongly influenced by the (n, α) ^{6}Li cross section, is modified by the presence of the sphere moderator.

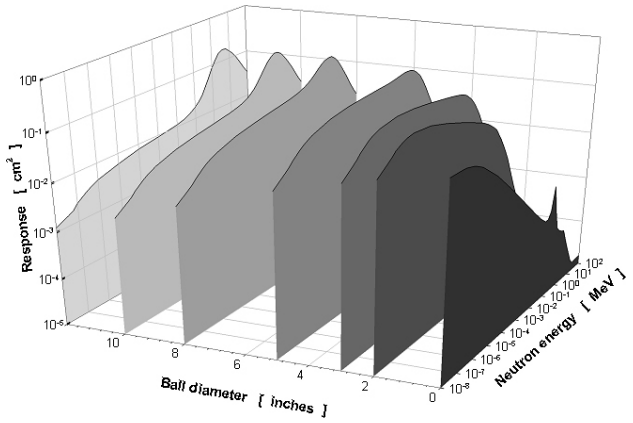

FIGURE 3. Energy interpolated response matrix for BSS with ^{6}LiI detector.

TABLE I. Energy-interpolated responses, in terms of (n, α) reactions per unit fluence, for each detector in function of neutron energy.

Neutron Energy [MeV]	Ball 0	Ball 2	Ball 3	Ball 5	Ball 8	Ball 10	Ball 12
1.000E-08	1.2442E-01	7.8124E-02	5.5369E-02	2.7185E-02	7.5199E-03	2.9188E-03	1.2280E-03
1.585E-08	1.2315E-01	8.9728E-02	6.4552E-02	3.1632E-02	8.6815E-03	3.3564E-03	1.3568E-03
2.512E-08	1.2189E-01	1.0305E-01	7.5256E-02	3.6806E-02	1.0022E-02	3.8595E-03	1.4989E-03
3.981E-08	1.2064E-01	1.1836E-01	8.7734E-02	4.2826E-02	1.1570E-02	4.4380E-03	1.6560E-03
6.310E-08	1.1917E-01	1.3659E-01	1.0292E-01	5.0120E-02	1.3445E-02	5.1459E-03	1.8587E-03
1.000E-07	1.1585E-01	1.6392E-01	1.2693E-01	6.1471E-02	1.6487E-02	6.3833E-03	2.3718E-03
1.585E-07	1.0876E-01	1.8124E-01	1.4784E-01	7.2431E-02	1.9509E-02	7.4842E-03	2.7539E-03
2.512E-07	1.0210E-01	2.0038E-01	1.7220E-01	8.5341E-02	2.3083E-02	8.7747E-03	3.1976E-03
3.981E-07	9.3393E-02	2.1360E-01	1.9288E-01	9.7585E-02	2.6379E-02	1.0008E-02	3.6351E-03
6.310E-07	8.3254E-02	2.1958E-01	2.0782E-01	1.0832E-01	2.9125E-02	1.1108E-02	4.0471E-03
1.000E-06	7.4218E-02	2.2572E-01	2.2392E-01	1.2022E-01	3.2155E-02	1.2329E-02	4.5055E-03
1.585E-06	6.2466E-02	2.2031E-01	2.2966E-01	1.2771E-01	3.4374E-02	1.3174E-02	4.7841E-03
2.512E-06	5.2576E-02	2.1503E-01	2.3554E-01	1.3566E-01	3.6746E-02	1.4077E-02	5.0798E-03
3.981E-06	4.4253E-02	2.0987E-01	2.4158E-01	1.4411E-01	3.9280E-02	1.5042E-02	5.3938E-03
6.310E-06	3.7245E-02	2.0484E-01	2.4777E-01	1.5309E-01	4.1991E-02	1.6073E-02	5.7273E-03
1.000E-05	3.1349E-02	1.9993E-01	2.5411E-01	1.6262E-01	4.4888E-02	1.7175E-02	6.0813E-03
1.585E-05	2.5368E-02	1.8733E-01	2.5069E-01	1.6730E-01	4.6721E-02	1.7916E-02	6.4028E-03
2.512E-05	2.0529E-02	1.7552E-01	2.4732E-01	1.7212E-01	4.8629E-02	1.8689E-02	6.7412E-03
3.981E-05	1.6613E-02	1.6446E-01	2.4399E-01	1.7708E-01	5.0614E-02	1.9495E-02	7.0975E-03
6.310E-05	1.3443E-02	1.5409E-01	2.4071E-01	1.8219E-01	5.2682E-02	2.0336E-02	7.4727E-03
1.000E-04	1.0879E-02	1.4438E-01	2.3747E-01	1.8743E-01	5.4833E-02	2.1213E-02	7.8677E-03
1.585E-04	8.6952E-03	1.3356E-01	2.2993E-01	1.8960E-01	5.6693E-02	2.1962E-02	8.1240E-03
2.512E-04	6.9499E-03	1.2356E-01	2.2264E-01	1.9178E-01	5.8616E-02	2.2736E-02	8.3886E-03

3.981E-04	5.5550E-03	1.1431E-01	2.1558E-01	1.9399E-01	6.0604E-02	2.3538E-02	8.6618E-03
6.310E-04	4.4397E-03	1.0575E-01	2.0874E-01	1.9623E-01	6.2661E-02	2.4368E-02	8.9439E-03
1.000E-03	3.5487E-03	9.7826E-02	2.0212E-01	1.9850E-01	6.4786E-02	2.5227E-02	9.2352E-03
1.585E-03	2.8353E-03	8.9779E-02	1.9441E-01	2.0014E-01	6.6815E-02	2.6149E-02	9.5611E-03
2.512E-03	2.2654E-03	8.2394E-02	1.8700E-01	2.0181E-01	6.8908E-02	2.7105E-02	9.8985E-03
3.981E-03	1.8101E-03	7.5618E-02	1.7987E-01	2.0348E-01	7.1066E-02	2.8095E-02	1.0248E-02
6.310E-03	1.4462E-03	6.9397E-02	1.7302E-01	2.0517E-01	7.3292E-02	2.9122E-02	1.0609E-02
1.000E-02	1.1600E-03	6.3592E-02	1.6621E-01	2.0680E-01	7.6152E-02	3.0428E-02	1.1086E-02
1.585E-02	9.3496E-04	5.8157E-02	1.5943E-01	2.0836E-01	7.9862E-02	3.2111E-02	1.1720E-02
2.512E-02	7.5359E-04	5.3188E-02	1.5292E-01	2.0993E-01	8.3753E-02	3.3888E-02	1.2391E-02
3.981E-02	6.2892E-04	4.7307E-02	1.4583E-01	2.1476E-01	9.0106E-02	3.6750E-02	1.3716E-02
6.310E-02	5.2911E-04	4.1803E-02	1.3888E-01	2.2049E-01	9.7521E-02	4.0110E-02	1.5347E-02
1.000E-01	5.3399E-04	3.5963E-02	1.3099E-01	2.2719E-01	1.0837E-01	4.6143E-02	1.7813E-02
1.585E-01	7.2000E-04	3.0528E-02	1.2200E-01	2.3403E-01	1.2268E-01	5.4817E-02	2.1285E-02
2.512E-01	2.2427E-03	2.5480E-02	1.0961E-01	2.3955E-01	1.4402E-01	6.8695E-02	2.7109E-02
3.981E-01	6.3412E-04	1.8553E-02	9.2248E-02	2.3682E-01	1.7010E-01	8.9786E-02	3.9078E-02
6.310E-01	2.2889E-04	1.3309E-02	7.5766E-02	2.2931E-01	1.9848E-01	1.1720E-01	5.6964E-02
1.000E+00	1.7938E-04	9.1081E-03	5.7610E-02	2.0795E-01	2.2278E-01	1.5233E-01	8.5974E-02
1.585E+00	1.5508E-04	5.9987E-03	4.1197E-02	1.7599E-01	2.3336E-01	1.8238E-01	1.1961E-01
2.512E+00	1.4230E-04	3.8493E-03	2.8283E-02	1.4218E-01	2.3324E-01	2.0659E-01	1.5746E-01
3.981E+00	8.3213E-05	2.2374E-03	1.8112E-02	1.0229E-01	2.0147E-01	2.0190E-01	1.7405E-01
6.310E+00	4.9620E-05	1.2896E-03	1.0934E-02	6.9649E-02	1.6069E-01	1.7831E-01	1.6997E-01
1.000E+01	3.0783E-05	7.5076E-04	6.6064E-03	4.5374E-02	1.1562E-01	1.3881E-01	1.4363E-01
1.585E+01	1.9090E-05	4.5407E-04	4.2394E-03	2.9868E-02	8.1086E-02	1.0446E-01	1.1666E-01
2.512E+01	1.4744E-05	2.8151E-04	2.4189E-03	1.8371E-02	5.5942E-02	7.6356E-02	8.8874E-02
3.981E+01	1.5393E-05	1.9549E-04	1.5624E-03	1.1967E-02	3.8106E-02	5.3770E-02	6.4948E-02
6.310E+01	1.5515E-05	1.5457E-04	1.1685E-03	8.5682E-03	2.6585E-02	3.7516E-02	4.6230E-02
1.000E+02	1.5413E-05	1.2360E-04	8.7244E-04	6.4118E-03	1.9577E-02	2.7399E-02	3.4316E-02

Uncertainties are $\leq 3\%$

In Figs. 4 to 10 are shown the Monte Carlo calculated, and their energy-interpolated values, response functions for Ball 0 to Ball 12, obtained in this study and those reported by Mares and Schraube.

In Fig. 4 can be noticed that there are differences. For this detector Mares and Schraube did the calculation irradiating the bare detector laterally while in this work all irradiations were carried out with the neutron disk source centered on and perpendicular to the axis of the central detector; also differences are attributed to the difference in the cross sections libraries utilized in both studies. In this response function can be noticed the influence of the ^{6}Li (n, α) cross section shown in Fig. 1.

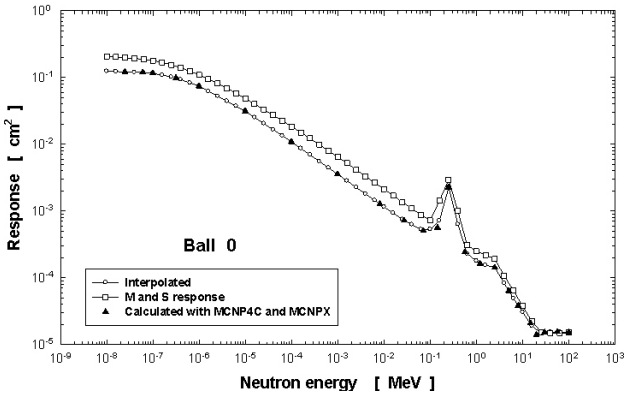

FIGURE 4. Calculated, interpolated and Mares and Schaube response function for bare detector.

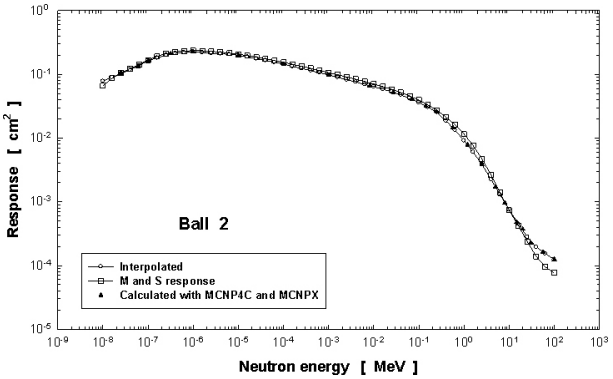

FIGURE 5. Calculated, interpolated and Mares and Schaube response function for Ball 2.

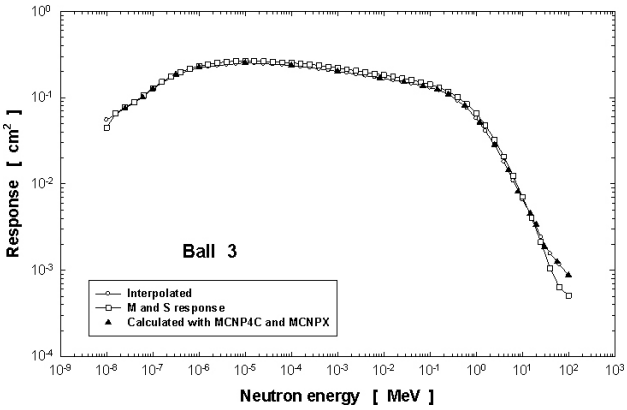

FIGURE 6. Calculated, interpolated and Mares and Schaube response function for Ball 3.

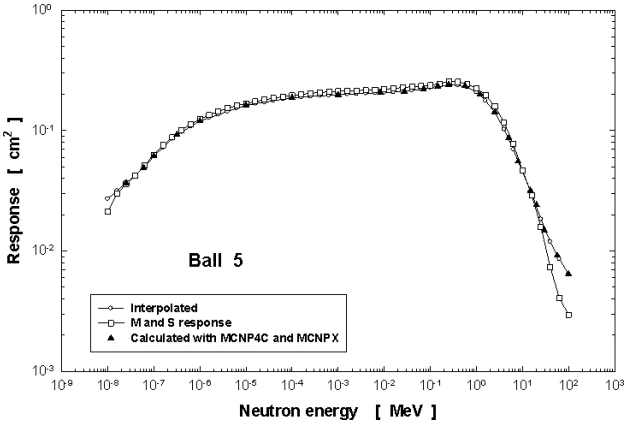

FIGURE 7. Calculated, interpolated and Mares and Schaube response function for Ball 5.

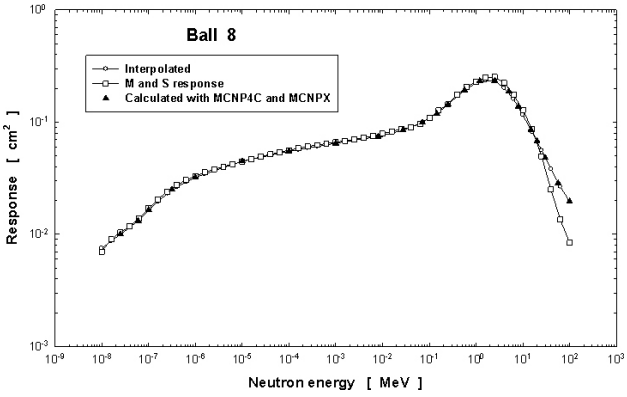

FIGURE 8. Calculated, interpolated and Mares and Schaube response function for Ball 8.

For Ball 2 to Ball 12 the main differences are in the low energy region and for neutrons whose energy is larger to 20 MeV, i.e. those values calculated using MCNPX. Probable explanation of this difference is attributed to the cross sections utilized by Mares and Schraube for neutrons beyond 20 MeV. They utilized the HIGH library [18], while in this study it was utilized those included in MCNPX.

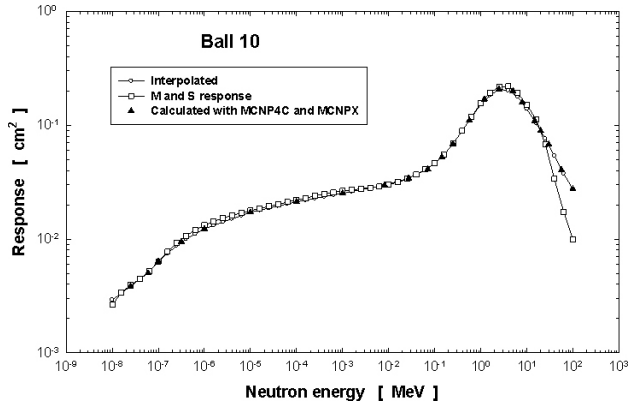

FIGURE 9. Calculated, interpolated and Mares and Schaube response function for Ball 10.

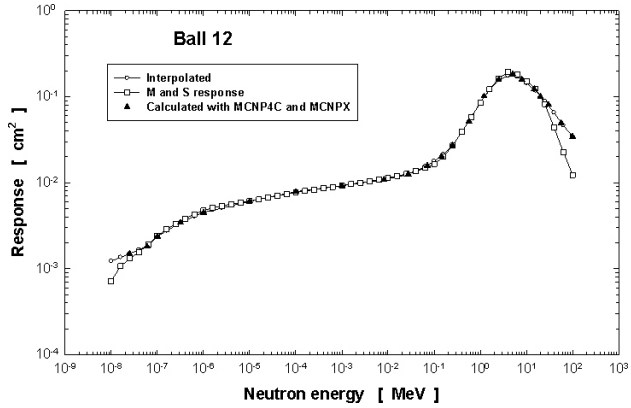

FIGURE 10. Calculated, interpolated and Mares and Schaube response function for Ball 12.

The χ^2 test was applied to compare the response functions with the Mares-and-Schraube's response functions. The test was applied using α = 0.95 and 22 degrees of freedom; for these parameters the χ^2-critical value is 12.338. The calculated chi-square values for each detector are shown in Table II. Using this test can be noticed that all the calculated chi-values are smaller than the critical chi-value. This means that there is not significant difference between the response functions calculated in this work and those reported by Mares and Schraube.

TABLE II. Calculated Chi-square.

Detector	χ^2
Ball 0	0.3312
Ball 2	0.0230
Ball 3	0.0437
Ball 5	0.0439
Ball 8	0.0449
Ball 10	0.0727
Ball 12	0.0798

4. Conclusions

The fluence responses for seven Bonner spheres have been calculated for neutrons from 2.50E(-8) to 100 MeV. The calculations have been performed using the MCNP 4C for neutrons from 2.50E(-8) to 20 MeV using the ENDF/B-VI cross-section library, while for neutrons between 30 to 100 MeV the response was obtained using the MCNPX code and the LA150 cross section library [23, 24]. For all the calculated cases with the spheres the S(α, β) scattering model was utilized during the transport of low energy neutrons.

Response matrix was calculated for 23 energy bins and the response functions were interpolated to include a larger number, 51, energy bins.

The response functions were compared with those reported by Mares and Schraube. Good agreement was also observed between our response matrix and the matrix calculated by other scientists. Response functions are similar in shape regardless of thermal neutron detector except for the B0 case where its response is strongly influenced by the type of thermal neutron detector.

Comparing the response function for B0 with the response function of Mares and Schraube differences are observed due to the irradiation conditions utilized during calculations and the cross sections libraries. For the other spheres the differences are mainly observed in the low energy region and in the case of neutrons whose energy is larger to 20 MeV; this is attributed to the different cross sections libraries utilized in both studies. The chi-square test was applied to determine if there are significant differences between our response functions and those reported by Mares and Schraube. From this test no significant differences were observed.

Acknowledgments

This work is part of the SYNAPSIS project supported by CONACyT (México) under contract SEP-2004-C01-46893.

∗ Correspondig author, e-mail: fermineutron@yahoo.com.

1. J. Chadwick, *Nature* **129** (1932) 312.
2. R.L. Bramblett, R.I. Ewing, and T.W. Bonner, *Nuclear Instruments and Methods* **9** (1960) 1.
3. F.D. Brooks and H. Klein, *Nuclear Instruments and Methods in Physics Research A* **476** (2002) 1.
4. M. Kralik *et al.*, *Radiation Protection Dosimetry* **70** (1997) 279.
5. A.V. Sannikov, V. Mares, and H. Schraube, *Radiation Protection Dosimetry* **70** (1997) 291.
6. V. Vylet, *Nuclear Instruments and Methods in Physics Research A* **476** (2002) 26.
7. E. Gallego, A. Lorente, and H.R. Vega-Carrillo, *Radiation Protection Dosimetry* **110** (2004) 73.
8. H.R. Vega-Carrillo, *Radiation Measurements* **35** (2002) 251.
9. J.E. Sweezy, N.E. Hertel, K.G. Veinot, R.A. and Karam, *Radiation Protection Dosimetry* **78** (1998) 263.
10. R. Barquero, R. Méndez, M.P. Iñiguez, H.R. Vega-Carrillo, and M. Voytchev, *Radiation Protection Dosimetry* **101** (2002) 493.
11. D.J. Thomas, A.G. Bardell, and E.M. Macaulay, *Nuclear Instruments and Methods in Physics Research A* **476** (2002) 31.
12. M.P. Dhairyawan, P.S. Nagarajan, and G. Venketaraman, *Nuclear Instruments and Methods* **175** (1980) 561.
13. A.V. Alevra and D.J. Thomas, *Radiation Protection Dosimetry* **107** (2003) 37.
14. B. Wiegel and A.V. Alevra, *Nuclear Instruments and Methods in Physics Research A* **476** (2002) 36.
15. H.R. Vega-Carrillo, E. Manzanares-Acuña, V.M. Hernandez-Dávila, and G.A. Mercado, *Rev. Mex. Fís.* **51** (2005) 47.
16. H.R. Vega-Carrillo *et al.*, *Rev. Mex. Fís.* **51** (2005) 494.
17. N.E. Hertel and J.W. Davidson, *Nuclear Instruments and Methods in Physics Research A* **238** (1985) 509.
18. V. Mares and H. Schraube, *Nuclear Instruments and Methods in Physics Research A* **337** (1994) 461.
19. H.R. Vega-Carrillo, B.W. Wehring, K.G. Veinot, and N.E. Hertel, *Radiation Protection Dosimetry* **81** (1999) 133.
20. BNL. [On line]. *Nacional Nuclear Data Center* http://www.nndc.bnl.gov; *Evaluated Nuclear Data File ENDF/B-VII.0 (USA, 2006)*. Brookhaven National Laboratory. [Consult: July 25^{th}, 2006].
21. J.F. Briesmeister, (editor), *MCNP^{TM}-A general Monte Carlo N-particle transport code*, *Los Alamos National Laboratory* ***Report LA-13709-M*** (2000).
22. J.S. Hendricks, S.C. Frankle, and J.D. Court, ENDF/B-VI Data for MCNP^{TM}, *Los Alamos National Laboratory* ***Report LA-12891*** (1994).
23. L.S. Waters, (editor), MCNPX User's manual version 2.4.0. *Los Alamos National Laboratory* ***Report LA-CP-02-408*** (2002).
24. M.B. Chadwick *et al.*, *Nuclear Science and Engineering* **131** (1999) 293.
25. E. Lemley, *Calculation of Bonner sphere neutron spectrometer response functions using the Monte Carlo computer code MCNP*, PhD dissertation, University of Arkansas (1996).
26. S.M. Seltzer and M.J. Berger, *International Journal of Applied Radiation and Isotopes* **33** (1982) 1189.